

Combining multiple optical trapping with microflow manipulation for the rapid bioanalytics on microparticles in a chip

G. Boer, R. Johann, J. Rohner, F. Merenda, G. Delacrétaz et al.

Citation: *Rev. Sci. Instrum.* **78**, 116101 (2007); doi: 10.1063/1.2804768

View online: <http://dx.doi.org/10.1063/1.2804768>

View Table of Contents: <http://rsi.aip.org/resource/1/RSINAK/v78/i11>

Published by the [American Institute of Physics](#).

Related Articles

Single-cell adhesion probed in-situ using optical tweezers: A case study with *Saccharomyces cerevisiae*
J. Appl. Phys. **111**, 114701 (2012)

Absolute calibration of optical tweezers including aberrations
Appl. Phys. Lett. **100**, 131115 (2012)

Three dimensional optical twistors-driven helically stacked multi-layered microrotors
Appl. Phys. Lett. **100**, 121101 (2012)

DNA-cisplatin binding mechanism peculiarities studied with single molecule stretching experiments
Appl. Phys. Lett. **100**, 083701 (2012)

Robust control approach to force estimation in a constant position optical tweezers
Rev. Sci. Instrum. **82**, 115108 (2011)

Additional information on Rev. Sci. Instrum.

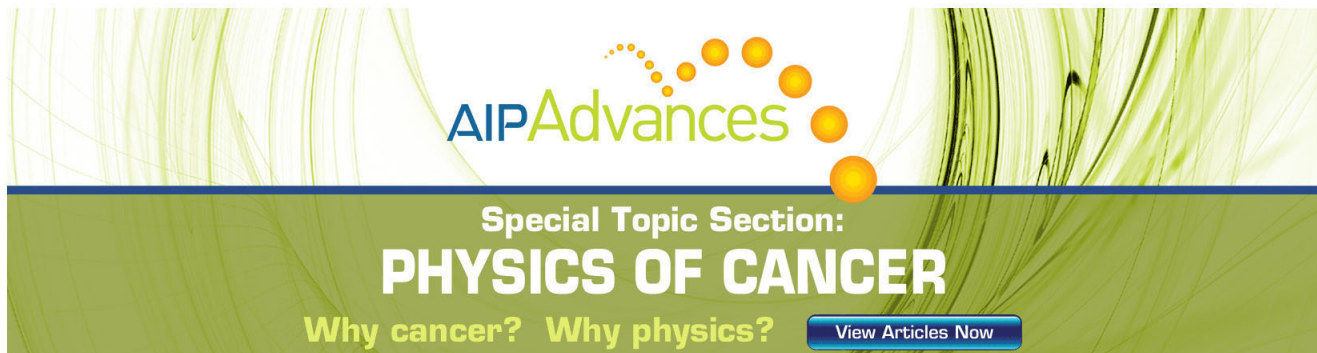
Journal Homepage: <http://rsi.aip.org>

Journal Information: http://rsi.aip.org/about/about_the_journal

Top downloads: http://rsi.aip.org/features/most_downloaded

Information for Authors: <http://rsi.aip.org/authors>

ADVERTISEMENT



AIPAdvances

Special Topic Section:
PHYSICS OF CANCER

Why cancer? Why physics? [View Articles Now](#)

Combining multiple optical trapping with microflow manipulation for the rapid bioanalytics on microparticles in a chip

G. Boer

ARCOptix S. A., Ch. Trois-Portes 18, NE-2000 Neuchâtel, Switzerland

R. Johann^{a)}

Fraunhofer-Institut für Biomedizinische Technik, IBMT, D-66386 St. Ingbert, Germany

J. Rohner, F. Merenda, and G. Delacrétaz

Laboratoire de Photonique Appliquée, Ecole Polytechnique Fédérale de Lausanne, EPFL, Station 17, CH-1015 Lausanne, Switzerland

Ph. Renaud

Laboratoire de Microsystème 4, Ecole Polytechnique Fédérale de Lausanne, EPFL, Station 17, CH-1015 Lausanne, Switzerland

R.-P. Salathé

Laboratoire de Photonique Appliquée, Ecole Polytechnique Fédérale de Lausanne, EPFL, Station 17, CH-1015 Lausanne, Switzerland

(Received 9 March 2007; accepted 10 October 2007; published online 14 November 2007)

An array of four independent laser traps is combined with a polydimethylsiloxane microfluidic chip to form a very compact system allowing parallel processing of biological objects. Strong three dimensional trapping allows holding objects such as functionalized beads in flows at speeds near 1 mm/s, enabling rapid processing. By pressure control of the inlet flows, the trapped objects can be put in contact with different solutions for analysis purpose. This setup, including a fluorescence excitation-detection scheme, offers the potential to perform complex biochemical manipulations on an ensemble of microparticles. © 2007 American Institute of Physics. [DOI: [10.1063/1.2804768](https://doi.org/10.1063/1.2804768)]

The study of the molecular mechanisms and dynamics underlying cell functions and creating “life” are in the center of system biology research.¹ Cell processes to be analyzed may be triggered by changing the composition of the cell environment. Ideally, in order to produce synchronous and equal signaling in the cell, all its surface is exposed at once to a definite concentration of the new medium. In practice, however, medium exchange proceeds through a gradual change in concentration. To accelerate the exchange and approach the ideal situation, the gradient slope needs to be made as steep as possible and the gradient region be passed as quickly as possible. The time scale of the medium exchange has to be much smaller than that of the molecular dynamics, which is in the range of 10^{-3} –1 s.¹ Parallel laminar flows seem to be a very suitable system for achieving rapid solution exchange. Different flows are well separated at short distance and the boundary between them can be sharpened by increasing flow speed. Hence, an adequate tool for cell handling needs to afford a strong force to enable the rapid movement of the cell between the fluids and to hold it against strong flows. We present a concept, where the phase exchange is performed by moving the phase boundary between laminar flows in a microdevice, while the cell is held in place by means of an optical tweezer. We use 2 μm polystyrene beads for evaluating the trapping force in place of cells. In other approaches, which are described rarely and very recently in the literature, the particle is shifted between

different fluids leaving the fluidics unchanged.^{2–4} With optical trapping a frequent method is to move the microscope stage with the chip having the optical path and particle position fixed.^{2,3} Although it is convenient, the large inertia of mass will limit high speed of short displacement. Here we see an advantage of our method.

For collecting many analytical data within reasonable time parallel processing with many traps is desirable. Methods for producing multiple traps, such as vertical cavity surface emitting lasers⁵ or diffractive optics,⁶ usually suffer from weak trapping forces due to the limited power per trap available and are therefore hardly applicable to high flow or particle displacement speeds. Our approach consists in a compromise combining several independent single tweezers, where each tweezer delivers a strong force, but where the creation of a large number of traps is not practical.

The instrumental setup of the combined system is sketched in Fig. 1. We used as a base an inverted microscope (Leica DM IRBE) equipped with a motorized x - y stage and a charge coupled device (CCD) camera. Four pigtailed monomode laser sources (Bookham Technology UC9), each of them delivering a maximal optical power of 100 mW at 974 nm, are arranged to form a trapping array. The collimated laser beams are injected with a set of dielectric mirrors via the fluorescence port of the microscope into a 100 \times oil immersion high-numerical aperture (NA) objective (Leica C-PLAN, NA of 1.25). The laser beams are tilted from each other by an angle of 0.8° to form in the front focal plane of the objective four traps in line with a 25 μm spacing. For optimal trapping strength, the diameter of the four collimated beams is adjusted to slightly overfill the rear pupil of the

^{a)} Author to whom correspondence should be addressed. Electronic mail: robert.johann@ibmt.fhg.de

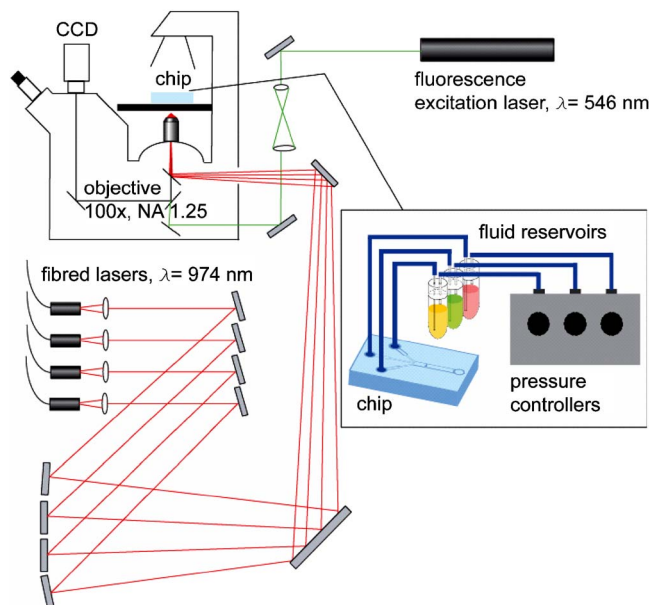


FIG. 1. (Color online) Optical trapping setup with integrated microfluidic system.

microscope objective. The focal length of the planoconvex collimation lenses at the exit of each pigtailed laser source was chosen to obtain collimated beams of 7 mm in diameter (for an irradiance drop of $1/e^2$), larger than the 6 mm rear pupil of the 100 \times objective. At the maximal laser output power of 100 mW, an estimated optical power of 40 mW is available at the focal plane of the microscope objective. In the present arrangement, the four traps are placed in line, however, any other array geometry can be formed, as well as the number of traps be increased by implementing additional laser sources. Fluorescence excitation is performed by introducing laser light of the desired wavelength via a side port of the inverted microscope. With the present setup fluorescence excitation is induced with a 0.5 mW HeNe laser source at 543 nm (Polytech GmbH). In order to allow fluorescence excitation over the whole imaging area, in other words at the four trapping sites, the excitation laser beam is decollimated before entering the microscope objective, in order to reach a diameter of roughly 100 μm in the plane of the optical traps. Observation is performed alternatively via a color CCD or a white gray CCD after proper filtering of the excitation wavelength and total rejection of the optical trap wavelength.

Catching and probing of the biological microobjects are performed within a 250 μm wide and 30 μm high central

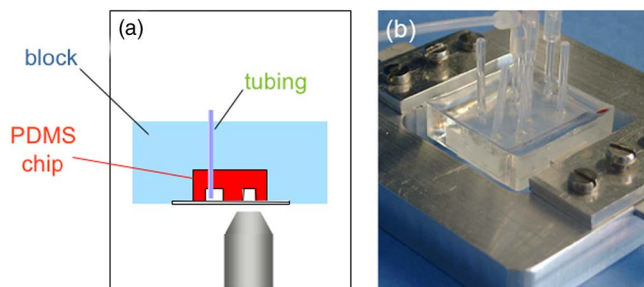


FIG. 2. (Color online) (a) PDMS chip and supply tubing encapsulated in transparent epoxy. (b) Used device (25 \times 25 mm²) mounted on a microscope adapter.

channel of a transparent polydimethylsiloxane (PDMS) chip with a 170 μm thick bottom glass plate. Three different liquids supplied from reservoir vessels by pressure are introduced through side channels. A partly filled reservoir is also connected to the chip outlet (not shown) to prevent flow instabilities due to fluid evaporation or unbalanced capillary forces. The chip is fabricated following a standard rapid prototyping procedure employing SU-8 photolithography for making the PDMS mold and oxygen plasma bonding for attaching the glass to the PDMS.⁷ The chip was cast in a block of hard and transparent epoxy [Fig. 2(a)], which serves as a rugged chip-to-world interface that stabilizes the fluid flows by fixing the supply tubes and enables chip mounting on the microscope by eliminating the danger of breaking the fragile chip glass, Fig. 2(b). For encapsulation, the chip with inserted supply tubes was first attached with the clean glass plate down on a flat sheet of PDMS. Thus the glass bottom is sealed and wetting by the epoxy is excluded. Then another piece of PDMS molded to the shape of a frame was attached to the PDMS sheet with the chip in the center.

PDMS is a suitable material for molds as it does not adhere to the epoxy. Liquid epoxy was finally poured in the frame to completely cover the chip and hardened for 1 day at RT. Encapsulation of the chip is assured by bonding of the epoxy to the free edge on the top side of the glass plate, which was originally chosen larger than the chip area. The epoxy resin was prepared from two components by mixing Epilox T 19-32/1000 (prepolymer) and Epilox M 835 (hardener) (Leuna-Harze GmbH, Leuna, Germany) at a 3:1 ratio (prepolymer:hardener) followed by degassing.

Fluid flows are controlled by means of three pressure regulators (Marsh-Bellofram, It's Us Ltd, UK), where one regulator is used for each fluid and chip inlet. The mechanical pressure regulators, which are supplied from a laboratory gas tap, allow for extremely smooth pressure control below a millibar. Flow handling is facilitated by setting a pressure offset positioning the fluid level of the exit reservoir above the levels of the entrance reservoirs.

The trapping strength was determined using the standard drag-force method,⁸ which consists in measuring the maximal viscous drag force withstood by a trapped bead without escaping the trap. This is practically done by maintaining the trap at a fixed position while moving the dish in which the

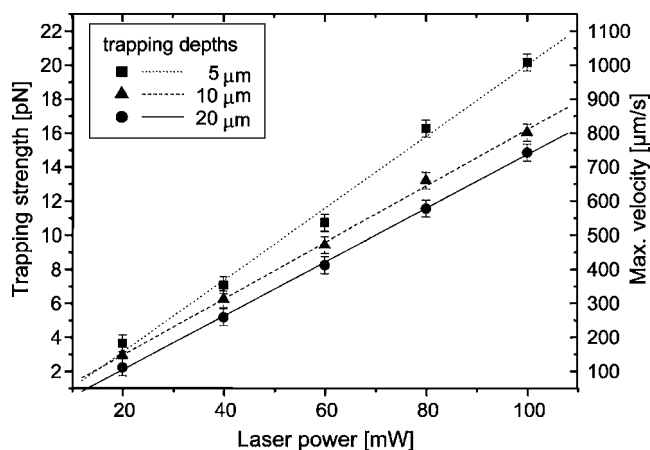


FIG. 3. Transverse trapping strengths of 2 μm diameter latex spheres as a function of the laser output power and trapping depth in water.

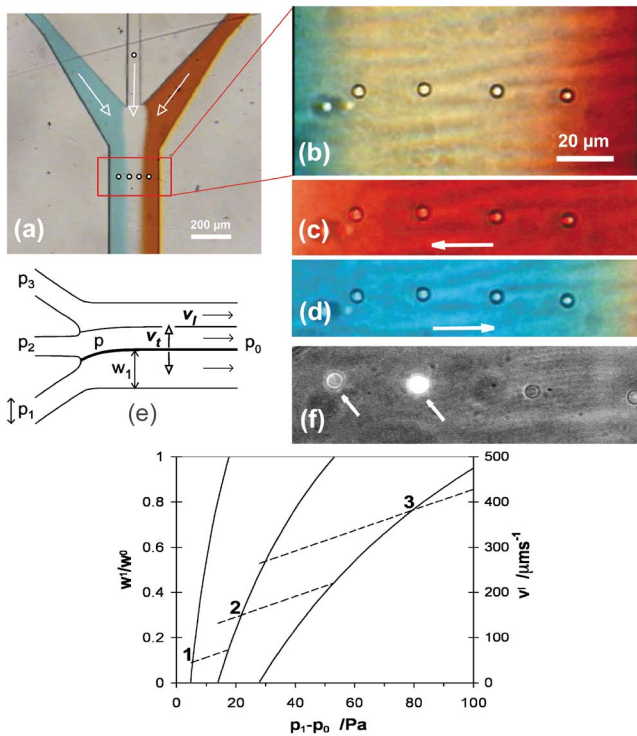


FIG. 4. (Color online) [(a)–(d)] Rapid flow switching in the microchip with trapped beads. For better visualization $5\ \mu\text{m}$ beads were chosen. (e) Modeling of flow switching (sketch and diagram). The width w_1 of a flow and the flow velocity v_1 , which is equal for all flows, can be derived as functions of the side channel inlet pressures p_1 , p_2 , and p_3 and the pressure on the exit p_0 from the flow equations $Q_i = v_i w_i h = (p_i - p) / R_i$ (i is the channel index, Q the volume flow rate, R the hydrodynamic resistance, and h the channel height, $30\ \mu\text{m}$) for the side channels and $v_i w_i h = (p - p_0) / R_0$ for the main channel under the constraint $w_0 = \sum w_i$ (w_0 is the main channel width, $250\ \mu\text{m}$):

$$v_i = \frac{p_i - p_0}{h(R_i w_i + R_0 w_0)},$$

and

$$\frac{w_1}{w_0} = \frac{(p_1 - p_0)R_2 R_3 + (p_1 - p_2)(R_2 + R_3)R_0}{(p_1 - p_0)R_2 R_3 + (p_2 - p_0)(R_2 + R_3)R_1}, \quad p_1, p_2 > p_0.$$

The diagram shows the variation of w_1 (solid curves) and v_1 (hatched lines) with the pressure $p_1 - p_0$ using the resistances (channel + 30 cm tubing) $R_1 = R_3 = 1.8 \times 10^{13}\ \text{kg s}^{-1}\ \text{m}^{-4}$, $R_2 = 2.0 \times 10^{13}\ \text{kg s}^{-1}\ \text{m}^{-4}$, $R_0 = 1.4 \times 10^{13}\ \text{kg s}^{-1}\ \text{m}^{-4}$ for constant and equal pressures $p_2 - p_0 = p_3 - p_0$. The curve (w_1/w_0 and v_1) pairs 1, 2, and 3 are for $p_2 - p_0 = 7.75$, 23.25, and 46.5 Pa, respectively. Each pressure ($p_{0..3}$) contains a hydrostatic pressure contribution of a reservoir. In practice the setting of the calculated v_1 and w_1 is not instantaneous due to the elasticity in the system. (f) Fluorescence detection allows to discriminate labeled beads ($\varnothing 4\ \mu\text{m}$, Molecular Probes A8858). Selected beads can be sorted downstream by individually switching the laser diodes. The trap distance is $25\ \mu\text{m}$.

bead is immersed at a constant speed using a computer controlled microscope stage. The maximal escape velocity v_{max} is determined by a stepwise increase of the stage velocity until the escape of the bead. The maximum drag velocity v_{max} at which the particle escapes the trap and the radial trapping force F_{trap} are related by Stokes law,⁹

$$v_{\text{max}} = \frac{F_{\text{trap}}(r)}{6\pi\eta r}, \quad (1)$$

where r is the bead radius and η is the viscosity coefficient of the medium. The trapping strength of our traps has been determined with $2\ \mu\text{m}$ polystyrene beads (Polysciences) held

at three different trapping depths (5, 10, and $20\ \mu\text{m}$) in water as a function of the laser output power (Fig. 3). At the maximal available output power of 100 mW, we found that the beads trapped at a depth of $10 \pm 2\ \mu\text{m}$ could withstand a maximal flow of $800\ \mu\text{m/s}$, which corresponds to a drag force of 16 pN. A decrease of the trapping force can be noticed when moving the trap deeper into the fluid. This is essentially due to the spherical aberrations caused by the refractive index mismatch between the immersion oil and the solution containing the beads. The increasing focal spot distortion with depth due to increased spherical aberrations is known to reduce the trapping efficiency.¹⁰

The immersion of the trapped objects in different fluid environments is demonstrated in Fig. 4. Figures 4(a) and 4(b) show a flow configuration with three parallel laminar streams and the trapping region with the four trapping sites spanning a distance of $100\ \mu\text{m}$ across the main channel. Flow speeds are adjusted from 0 to $150\ \mu\text{m s}^{-1}$. The objects trapped are $5\ \mu\text{m}$ diameter polystyrene beads introduced with the solution in the middle. Trapped beads can be rapidly exposed to one of the side flows by abruptly increasing the flow rate of the liquid, Figs. 4(c) and 4(d). The liquid exchange process is accompanied by the parallel shifting of the flow boundary across the channel, dipping the particles one by one in the new fluid. The position of the boundary in dependence of the pumping pressures is illustrated in Fig. 4(e). The minimal time required for immersing all the beads ($100\ \mu\text{m}$ distance) can be derived for $2\ \mu\text{m}$ beads from Fig. 3. When trapping with 100 mW at half the channel height, the maximal applicable flow speed $v_f (= dw_1/dt)$ of the boundary is nearly $800\ \mu\text{m s}^{-1}$, which corresponds to an immersion time of $1/8\ \text{s}$. However, in practice, this time is higher due to the elasticity in the system (from PDMS chip, tubes, gas volumes). In order not to lose the beads during flow switching, v_1 has to be adjusted below $800\ \mu\text{m s}^{-1}$, since it increases with w_1 [see Fig. 4(e)]. The possibility of dipping only part of the particles with this method by stopping the flow boundary between two beads is favored by high flow rates which keep diffusive mixing of the flows at the boundary low. The applicability of high flow rates also diminishes sedimentation and attachment of the beads to the channel bottom, before they enter the traps.

The authors wish to thank the Swiss Commission for Technology and Innovation for its support (Grant Nos. CTI 6633.1 TNS-NM and 6983.1 KTS-NM). We also would like to thank J. M. Fournier for stimulating discussions.

- ¹D. N. Breslauer, P. J. Lee, and L. P. Lee, *Mol. BioSyst.* **2**, 97 (2006).
- ²E. Eriksson, J. Enger, B. Nordlander, N. Erjavec, K. Ramser, M. Goksör, S. Hohmann, T. Nyström, and D. Hanstorp, *Lab Chip* **7**, 71 (2007).
- ³J. Enger, M. Goksör, K. Ramser, P. Hagberg, and D. Hanstorp, *Lab Chip* **4**, 196 (2004).
- ⁴U. Seger, S. Gawad, R. Johann, A. Bertsch, and Ph. Renaud, *Lab Chip* **4**, 148 (2004).
- ⁵M. Ozkan, M. Wang, C. Ozkan, R. Flynn, A. Birkbeck, and S. Esener, *Biomed. Microdevices* **5**, 61 (2003).
- ⁶E. R. Dufresne and D. G. Grier, *Rev. Sci. Instrum.* **69**, 1974 (1998).
- ⁷D. C. Duffy, J. Mc Donald, O. J. A. Schueller, and G. M. Whitesides, *Anal. Chem.* **70**, 4974 (1998).
- ⁸W. H. Wright, G. J. Sonek, and M. W. Berns, *Appl. Opt.* **33**, 1735 (1994).
- ⁹J. Happel and H. Brenner, *Low Reynolds Number Hydrodynamics*, 2nd ed. (Kluwer, Dordrecht, 1991), p. 553.
- ¹⁰H. Felgner, O. Muller, and M. Schliwa, *Appl. Opt.* **34**, 977 (1995).